

ANDRZEJ OSAK*

STUDIES OF ELECTRICAL TRANSPORT
IN BARIUM TITANATE SINGLE CRYSTALBADANIE ZJAWISK TRANSPORTU ELEKTRYCZNEGO
W MONOKRYSTALE TYTANIANU BARU

Abstract

Results of the studies on electrical transport and related relaxation phenomena in ferroelectric BaTiO₃ single crystal are presented. Investigations of polarisation and depolarisation in the samples show an existence of very slow relaxation currents in the material. In the neighbourhood of Curie temperature the relation $J \sim V^{6.5}$ is fulfilled. The energy activation calculated from depolarisation currents and electrical conductivity are the same and equal to 0.42eV.

Keywords: ferroelectrics, J-V characteristics

Streszczenie

W artykule zostały przedstawione wyniki badań nad przewodnictwem elektrycznym i mechanizmem relaksacji w ferroelektrycznym monokryształe BaTiO₃. Badania polaryzacji i depolaryzacji w tym materiale wskazują na występowanie bardzo wolnych prądów relaksacji. W pobliżu punktu Curie spełniony jest związek $J \sim V^{6.5}$. Energie aktywacji wyznaczone z prądów depolaryzacji i przewodnictwa elektrycznego są takie same i równe 0,42eV.

Słowa kluczowe: ferroelektryki, charakterystyki J-V

* Dr inż. Andrzej Osak, Instytut Fizyki, Wydział Fizyki, Matematyki i Informatyki Stosowanej, Politechnika Krakowska.

1. Introduction

The charge transport in ferroelectric oxides having perovskite (barium titanate) or perovskite-related structures can have important effects on device performance. The type and concentration of charge carriers in the crystal of barium titanate are determined by the defect chemistry and are affected by temperature, the oxygen pressure and the concentration of dopant [1–5]. The measurements of the J-V characteristics is a very useful method for charge transport investigations.

Studies of the current – voltage (J-V) characteristics in barium titanate were reported in many papers. The J-V characteristics in single BaTiO₃ crystals [6–15], polycrystals [16–18] and in doped single crystals [19–28] were investigated. Many researches referred to doped polycrystalline barium titanate in which a high positive temperature coefficient of the resistivity (PTC) was discovered [19–26]. In spite of many studies performed on the J-V characteristics, there are also some problems which need further studies. One of the most essential is a question, to what extent one can apply the theory of space charge limited currents (SCLC) [31, 32] to explain a shape of the J-V characteristics in ferroelectric crystals. It is well known that, after applying the step polarisation voltage in a dielectric sample, relaxation currents flow (see for example [29, 30]). There also arise a question, how much relaxation currents which appear in ferroelectric crystals, may influence the J-V characteristics. In this paper some results of our studies on these problems are presented.

2. Theory

2.1. Space charge limited current in linear dielectrics

Theory of space charge limited currents in linear dielectrics was presented in the many monographs (see for example [31, 32]). It is known that the space charge limited currents appear in dielectrics when the two following conditions are satisfied:

- (1) ohmic electrodes are deposited on the sample;
- (2) there are more injected excess carriers than thermally generated ones.

According to the SCLC theory, a relation between an applied voltage and a current flowing through the sample depends on:

- (1) value of the applied voltage V ,
- (2) density of the traps N_t ,
- (3) distribution of the trap energy levels E_t in the forbidden gap,
- (4) thickness of the sample d .

For dielectrics without traps (trap free case), in weak electric fields, Ohm's law holds

$\left(J \propto \frac{V}{d} \right)$, while in higher fields, Mott–Gurney–Child's law $\left(J \propto \frac{V^2}{d^3} \right)$ is fulfilled. For

crystals in which the traps are distributed exponentially within the forbidden energy gap, as

Mark and Helfrich have shown [31], the following relation should be valid: $J \propto \frac{V^{l+1}}{d^{2l+1}}$,

where: $l = T_t/T$ and T_t is a constant characteristic for a given trap energy distribution.

For crystals with an ununiform trap energy distribution within the forbidden energy gap, as Rose, Hwang, Kao and Miller have shown [32], the current is an exponential function of the voltage: $J \propto \exp\left(\frac{V}{d^2}\right)$.

The shape of the J-V characteristics depends also on temperature, a variation of which changes both density n and mobility of the charge carriers μ .

All really observed J-V characteristics are inserted inside Lampert's. Triangle [31], as shown in Fig. 1

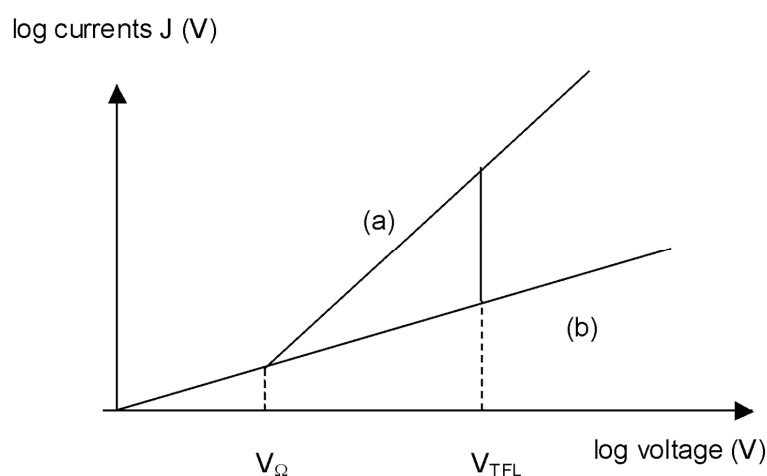


Fig. 1. Lampert's triangle
Rys. 1. Trójkąt Lamperta

When the density of thermally generated free carriers inside of sample is larger than the density of injected carriers the ohmic conduction predominant. The onset of the transition from the ohmic to SCL conduction occurs when the applied voltage reaches the value of V_{Ω} . The value of V_{Ω} increases with increasing of trap concentration. When all traps are filled up, the injected carriers will be free to move in the sample so that at the threshold voltage V_{TFL} the current will rapidly jump up from its low trap limited value to a high trap free SCLC current. The V_{TFL} is defined as voltage required to feel the traps.

2.2. Ferroelectric crystals

The ferroelectric crystals have a great dielectric permittivity and simultaneously a very low electrical conductivity. This is why, one can expect in these materials a presence of the space charge limited currents [6–8]. In ferroelectrics, a description of these currents is much more complicated than in linear dielectrics. The reason is that in the case of the ferroelectric materials a dielectric polarisation is not a linear function of the applied electric field strength and the dielectric permittivity strongly depends on temperature. In calculations, one must consider a relation between the polarisation and applied electric field which is

$$E = \alpha P + \beta P^3 + \gamma P^5, \quad (1)$$

where α , β and γ are Devonshire's coefficients; P denotes the polarisation of the sample and E is the electric field related to the applied voltage through the dependence

$$V = \int_0^d E(x) dx. \quad (2)$$

The current flowing through the sample is a sum of drift and diffusion currents

$$J = e\mu n E + eD \frac{\delta n}{\delta x} \quad (3)$$

where e is the charge of carriers, μ is carriers mobility, n – free carriers concentration and D – diffusion constants.

For the quantities appearing in eqs. (1)–(3), the Poisson's equation holds

$$\frac{dP}{dx} = en \quad (4)$$

The set of equations (1)–(4) has been solved under assumption that the trapping may be neglected and that the thermally activated equilibrium concentration of the carriers equals zero. Fridkin and Kreher [33], for the ferroelectrics with the phase transition of the first order (barium titanate) in the range of the temperatures near Curie temperature T_c , showed that the following dependencies are true:

– for the strong fields

$$J = 0.36\gamma^{-1/5}\mu \frac{V^{6/5}}{d^{11/5}}, \quad (5)$$

– for the weak fields

$$J = \frac{9}{8}\mu\epsilon^{-1} \frac{V^2}{d^3}, \quad (6)$$

which is Mott–Gurney–Child's law.

3. Results

3.1. Experimental method

Details of the experimental set up were described in [35]. Very weak polarisation and depolarisation currents (down to 10^{-13} A) were measured using a Vibron Dynamic Electrometer, type VJ-51.1, of the sensibility down to 10^{-16} A. The measured currents were of the magnitude of three orders greater than the sensibility of the electrometer. The temperature controller, type 650H Unipan, allowed to control the temperature of the sample with an accuracy better than $0,01^\circ\text{C}$.

Prior to each measurement, the temperature of the sample was risen up to 150°C (i.e. above the Curie temperature). The sample was kept for 1 hour at this temperature and then cooled to the required temperature.

3.2. Samples

The barium titanate single crystals were grown using Remeika's technique. The samples were 0.3 mm thick. The surface area of the electrodes varied between 3 and 7 mm². The J-V characteristics were measured on sample with indium electrodes whereas the dielectric permittivity and electrical conductivity with gold electrodes. Indium and gold electrodes were deposited by evaporation in vacuum.

3.3. Dielectric permittivity

Dielectric permittivity was measured for temperatures varying between 20 and 180°C using Tesla Bridge, type BM 595. The frequency of the measuring field was 1000 Hz and the probing voltage was 1V. Fig. 2 shows the shape of the two following dependencies: $\epsilon(T)$ – curve 1 and $1/\epsilon(T)$ – curve 2. It follows from the data that the Curie temperature T_c equals $131 \pm 0.5^\circ\text{C}$, the Curie point T_0 is $119 \pm 0.5^\circ\text{C}$ and the Curie-Weiss constant C assumes the value $1.56 \times 10^5 \text{C}$.

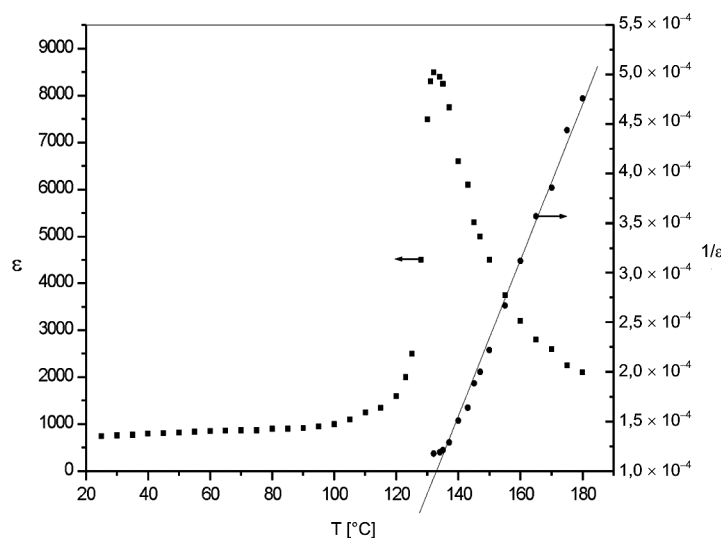


Fig. 2. Temperature dependence of dielectric permittivity
Rys. 2. Zależności przenikalności elektrycznej od temperatury

3.4. Charging currents

Charging currents were measured in the ferroelectric phase (temperatures lower than 131°C) and in the paraelectric phase (temperatures higher than 131°C). The charging currents at 25, 75 and 125°C are shown in Figs 3a, 3b and 3c respectively, whereas in Fig. 3d charging currents measured in paraelectric phase (140°C) are presented. The results show that, at low voltages, the charging currents reach steady state values after a long time (10^4 – 10^5 s). In this case, some special precautions have been undertaken to eliminate a drift in the measuring electronic systems. At higher temperatures and higher polarisation voltages, the steady state currents have been reached in shorter times (10^3 s).

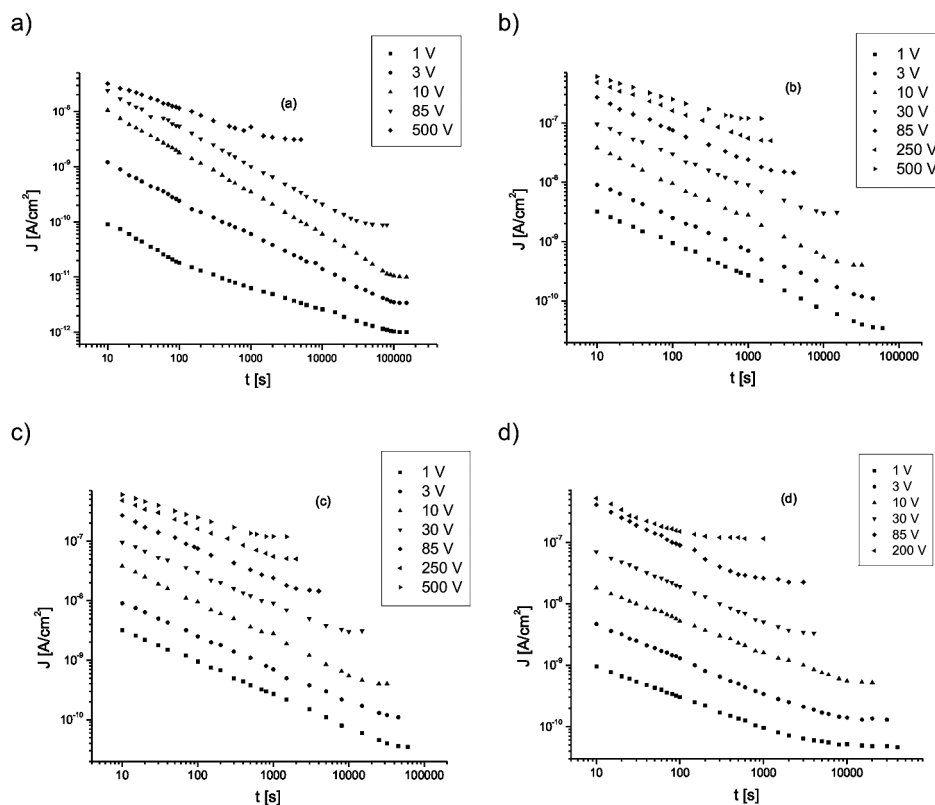


Fig. 3. Charging currents measured at four chosen temperatures: a) 25°C, b) 75°C, c) 125°C, d) 140°C. The polarisation voltage is indicated on each curve
 Rys. 3. Prądy ładowania dla czterech wybranych temperatur: a) 25°C, b) 75°C, c) 125°C, d) 140°C. Napięcie polaryzacji zostało podane przy każdej krzywej

3.5. The J-V characteristics

The values of the charging currents measured 10, 10^2 and 10^3 s after application of the voltage as well as steady state current values have been used to plot a set of the J-V characteristics (isochroms). In Fig. 4, there are shown the J-V characteristics measured at 125°C, i.e. close to the Curie temperature after various times of application of the polarisation voltage.

As time increases, the shape of the isochrom J-V characteristics become more and more similar to the J-V characteristics measured after polarisation time t_s . Fig. 5 shows the J-V characteristics measured at chosen temperatures 25, 75, 125 and 140°C.

The values of the steady state charging currents I_s obtained after polarisation time t_s have been used to plot J-V characteristics. The polarisation time t_s depends on temperature and electric field strength.

The following conclusions result from the obtained data:

– for low voltages, independently temperature, Ohm's law is fulfilled;

- for high voltages and at temperatures far from the Curie temperature (25 and 140°C), Mott–Gurney–Child’s law holds ($J \propto V^2$), whereas at temperatures close to the Curie temperature (125°C) the dependence between J and V follows a power law: $J \propto V^{1.21}$. This result proves an earlier theoretical result obtained for ferroelectrics with the first order phase transition (see formula (5));
- for intermediate fields, the slope of the J - V curve increases from 1.28 at 25°C to 1.96 at 125°C.

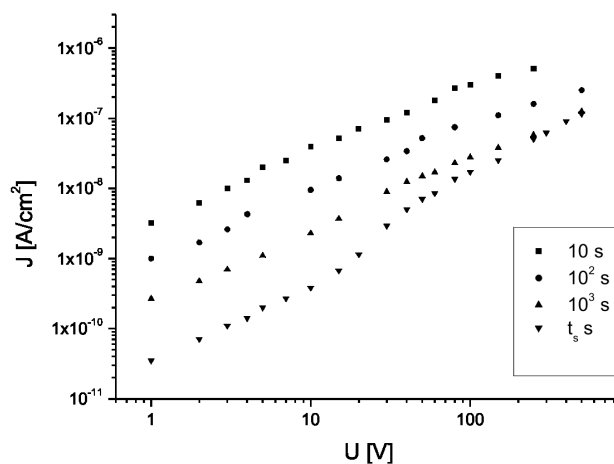


Fig. 4. J-V characteristics measured after various times of application of the voltage (isochrom curves) at temperature 125°C: 10 s (curve 1), 10²s (curve 2), 10³ s (curve 3), t_s – in steady state (curve 4)

Rys. 4. Charakterystyki prądowo napięciowe zmierzone po upływie różnych czasów od przyłożenia napięcia w temperaturze 125°C: 10 s (krzywa 1), 10²s (krzywa 2), 10³ s (krzywa 3), t_s – stan ustalony (krzywa 4)

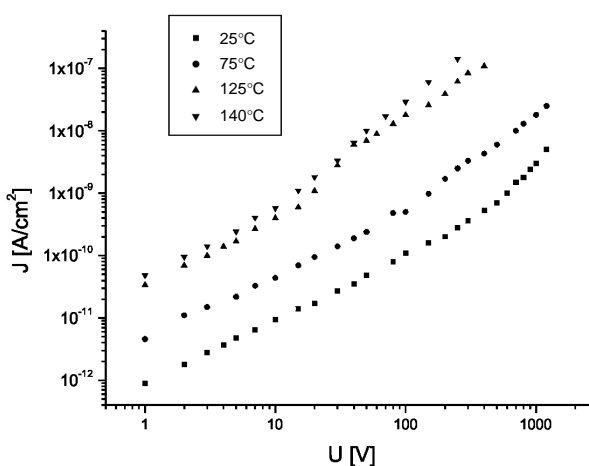


Fig. 5. J-V characteristics measured at various temperatures: 140°C (curve 1), 125°C (curve 2), 75°C (curve 3), 25°C (curve 4)

Rys. 5. Charakterystyki prądowo napięciowe wyznaczone w temperaturach: 140°C (krzywa 1), 125°C (krzywa 2), 75°C (krzywa 3), 25°C (krzywa 4)

The J-V characteristics follow the power law $J = AV^n$, with A and n values yielded by the power regression method as listed in Table I.

Table 1

A and n values yielded by the power regression method

Temperature	Voltage range	Regression coefficient and errors		
		A	n	r
25°C	1–150V	$9.11 \pm 0.31 \times 10^{-12}$	1.01 ± 0.03	0.998
	200–500V	$2.25 \pm 0.12 \times 10^{-13}$	1.28 ± 0.08	0.978
	500–1500V	$8.37 \pm 0.53 \times 10^{-16}$	2.10 ± 0.11	0.994
75°C	1–100V	$4.97 \pm 0.27 \times 10^{-12}$	0.97 ± 0.04	0.997
	100–300V	$1.56 \pm 0.85 \times 10^{-13}$	1.75 ± 0.08	0.991
	300–1500V	$2.16 \pm 0.14 \times 10^{-12}$	1.63 ± 0.07	0.996
125°C	1–15V	$3.43 \pm 0.16 \times 10^{-11}$	1.05 ± 0.04	0.997
	15–60V	$4.07 \pm 0.20 \times 10^{-11}$	1.96 ± 0.08	0.996
	80–500V	$7.02 \pm 0.43 \times 10^{-11}$	1.21 ± 0.05	0.998
140°C	1–10V	$4.17 \pm 0.21 \times 10^{-11}$	1.11 ± 0.05	0.998
	15–500V	$1.08 \pm 0.06 \times 10^{-11}$	1.96 ± 0.09	0.997

3.6. Electrical conductivity

D.c. electrical conductivity was measured in the range of temperatures from 20 to 150°C. The probing voltage, equal to 10V, was chosen so that Ohm's law to be valid. The measurements were performed in the cooling process at the rate 10°C per hour. Programmable temperature controller, type 680 Unipan, was used to control the rate of the cooling. Fig. 6 shows the temperature dependence of the electrical conductivity.

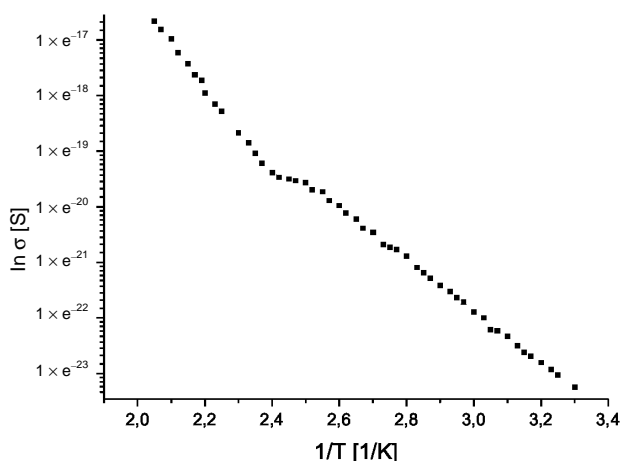


Fig. 6. Temperature dependence of d.c. electrical conductivity
Rys. 6. Zależność stałoprądowego przewodnictwa elektrycznego od temperatury

The electrical conductivity $\sigma(T)$ changes with temperature according to the Arrhenius law $\sigma = \sigma_0 \exp\left(-\frac{B}{T}\right)$ both in ferroelectrics and paraelectric phases. The activation energies calculated separately above and below the Curie temperature by the exponential regression method are listed in Table 2. In the ferroelectric and paraelectric phases, activation energies are: 0.41 eV and 0.62 eV respectively.

Table 2

The activation energies calculated above and below the Curie temperature

Temperature	$T < T_c$	$T > T_c$
σ_0	$(4.94 \pm 0.27) \times 10^{-4} \Omega^{-1} \text{m}^{-1}$	$(0.69 \pm 0.04) \times 10^{-4} \Omega^{-1} \text{m}^{-1}$
E	$(0.41 \pm 0.03) \text{ eV}$	$(0.62 \pm 0.04) \text{ eV}$
r	0.996	0.998

3.7. Isothermal depolarisation currents

The samples have been polarised for half an hour using the electric field 33 kV/m. After poling, the samples have been discharged at the same temperature. Fig. 7 shows, in the log-log scale, a typical set of the discharging currents for chosen temperatures. The integration of the discharging current $\left(\int I_c dt\right)$ has allowed to calculate the total depolarisation charge Q . Its initial value was measured by means of an electrometer Unipan type 219. In the insert of Fig. 7, there is shown a shape of the dependence between $\ln Q$ and $1/T$. The activation energy evaluated by the exponential regression method equals $(0.42 \pm 0.02) \text{ eV}$.

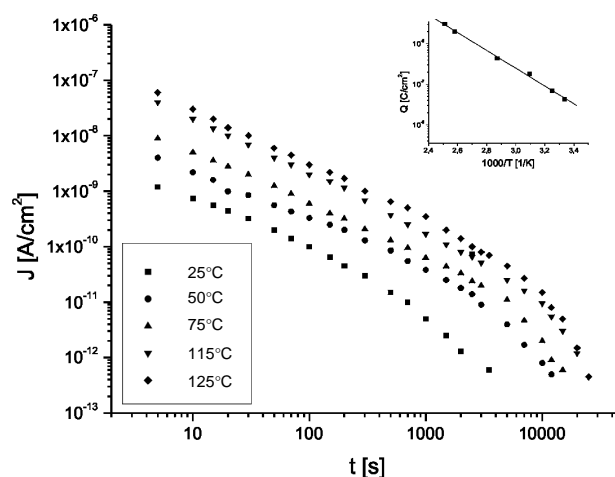


Fig. 7. Discharging currents at various temperatures for the sample polarised with the voltage 10 V. Polarisation time 30 minutes: 125°C (curve 1), 115°C (curve 2), 75°C (curve 3), 50°C (curve 4), 25°C (curve 5). In Insert: $\log Q$ versus $1/T$

Rys. 7. Prądy rozładowania w różnych temperaturach dla próbek spolaryzowanych pod napięciem 10 V. Czas polaryzacji 30 minut: 125°C (krzywa 1), 115°C (krzywa 2), 75°C (krzywa 3), 50°C (krzywa 4), 25°C (krzywa 5). Wykres wklejony: Zależność $\log Q$ od $1/T$

4. Discussion

1. The electric field applied to the sample causes:

- 1) change of the ferroelectric domain configuration;
- 2) displacement of free and localised carriers.

The changes of the domain structure are due to both the movement of the existing domains and the nucleation of new ones. A rate of both processes depends on the electric field strength and temperature. In weak electric fields (about 200 V/cm), as Wieder's results have shown [36], the polarisation process can persist even several hours. The bulk free charges and those injected from the electrodes undergo the localisation due to trapping and screening of the spontaneous polarisation. Therefore a number of free charges decreases with time and the system relaxes towards equilibrium in which only the d. c. conductivity current flows through the sample (see Fig. 3a, 3b, 3c, and 3d).

Prior to the attainment of the steady state, immediately after application of the electrical field, many various current transients may occur. A decay of the space charge limited transient current is rather rapid [32]. In turn, the transient current connected with the movement of the domains decays rather slowly, especially at low and intermediate fields. Therefore, for longer times, the total charging transient current is determined rather by the rate of the domains movement.

2. The steady state charging currents I_s have been used to plot the J-V characteristics at various temperatures (see Fig. 5). Barium titanate possesses the spontaneous polarisation, therefore some peculiarities in the SCL current in ferro- and paraphases may be observed. The obtained results really show some differences in SCL currents in ferro- and paraphase (see Fig. 5). The J-V characteristics have been studied at temperatures far from the Curie temperature (25, 75 and 140°C) and at a temperature chosen close to the Curie temperature (125°C). As it has been stated, the J-V characteristics at low temperatures measured at 25 °C, satisfied Ohm's law. For higher voltages, Mott–Gurney–Child's square law approximately holds (see Fig. 5, curve 4). These results are characteristic for linear dielectrics. At low applied voltages, the J–V characteristics follows Ohm's law, because the density of thermally generated free carriers inside the specimen is predominant. The onset of the departure from Ohm's law (the onset of SCL conduction) takes place when the density of thermally generated free carriers is lower than density of carriers injected from the electrode. At low temperatures, the ferroelectric properties do not essentially influence the shape of J-V characteristics at higher voltages. At 125°C, which is close to the Curie temperature, the relation $J \propto V^{1.22} \approx V^{6/5}$ holds, typical for ferroelectrics with the first order phase transition, has been found. For ferroelectrics, close to the Curie temperature in accordance with the SCL theory [33, 34], the non-linear terms in eq. (1) are of special importance (especially at higher polarisation voltages). In this case the relation $J \propto V^{1.22}$ should be satisfied as it really follows from the measurements. It is seen in Fig. 5 that transition voltage from the ohmic to the SCL conduction decreases with increasing temperature (from 200V at 25°C to 15V at 140°C). At low temperatures below the Curie temperature there is a significant trapping of carriers (injected and thermally generated) at the domain walls and imperfections of crystal structure. At higher

temperatures (above the Curie temperature) spontaneous polarisation disappears. Trapping at domain walls vanishes and simultaneously at high temperatures the thermal release of trapped carriers become much faster. That is why at 140°C the SCL conduction is predominant and at lower voltage the Ohmic conduction is suppressed.

3. The activation energies calculated from the temperature dependence of the electrical conductivity are equal 0.41 eV and 0.62 eV in para- and ferroelectric phases, respectively. The same activation energies were obtained in earlier papers [37]. The activation energy calculated from the temperature dependence of the depolarisation charges in ferroelectric phase also equals 0.42 eV (Fig. 6). The same equality of the activation energies relation was earlier found in other materials [38–41].

The barium titanate single crystals grown by Remeika's method show some amount of oxygen vacancy defects (O^{2-}). A migration of carriers between the long-range potential centres associated with the defects is a basic transport mechanism both in the case of current conduction and dielectric polarisation. The loss of oxygen causes a creation of the Ti^{3+} ions in the structure. This, in turn, influences the electrical conductivity as the conduction in $BaTiO_3$ is predominantly through the electron hopping from Ti^{4+} to Ti^{3+} sites. The polarisation occurs for certain specific types of paths between the sites. There may be some linear chains, along which the potential barriers are almost identical for the whole chain, and the electrons can easily pass from one electrode to another and contribute to the d. c. conductivity. There also may be other chains containing large wells. The electrons cannot pass the well and the dipole polarisation may arise from the confinement of electrons between these large potential barriers.

5. Conclusions

1. In barium titanate single crystal, at temperatures below the Curie temperature, very slow depolarisation currents flow.
2. At low voltages, Ohm's law is fulfilled both in para- and ferroelectric phases.
3. In the ferroelectric phase, for intermediate voltages, the relation $J \propto V^n$ is valid with the power n increasing as temperature increases: from 1.37 at 25°C to 1.96 at 125°C.
4. For both intermediate and high voltages, in the vicinity of the Curie temperature, the shape of J-V characteristics changes in agreement with SCL theory for ferroelectrics with the first order phase transition.

References

- [1] Seuter A.M., *Defect Chemistry and Electrical Transport Properties of Barium Titanate*, Philips Res. Repts Suppl. **4**, 1973, 1-84.
- [2] Nowotny J., Rekas M., *Defect Structure and Electrical Properties of Barium Titanate*, Key Engineering Materials **66-67**, 1992, 1-44.
- [3] Kim I.Y., Song C.H., Yoo H.I., *Mn-doped $BaTiO_3$ Electrical Transport Properties in Equilibrium State*, Journal of Electroceramics **1**, 1997, 27-39.
- [4] Smyth D.M., *Ionic Transport in Ferroelectrics*, Ferroelectrics **151**, 1994, 115-124.

- [5] Waser R., *Charge Transport in Perovskite-type Titanates: Space Charge Effects in Ceramics and Films*, *Ferroelectrics* **151**, 1994, 125-131.
- [6] Branwood A., Tredgold R.H., *The Electrical Conductivity of Barium Titanate Single Crystals*, *Proc. Phys. Soc.* **76**, 1960, 93-98.
- [7] Branwood A., Hughes O.H., Hurd J.D., Tredgold R.H., *Evidence for Space Charge Conduction in Barium Titanate Single Crystals*, *Proc. Phys. Soc.* **79**, 1962, 1161-65.
- [8] Roberts G.G., Tredgold R.H., *Space Charge Injection into Impurity Semiconductors*, *J. Phys. Chem. Solids* **24**, 1963, 1263-56.
- [9] Roberts G.G., Tredgold R.H., *Space Charge Injection into Impurity Semiconductors II*, *J. Phys. Chem. Solids* **25**, 1964, 1349-56.
- [10] Siniakov E.V., Kudzin A.J., *Anomalia elektroprovodimosti monokristalov titanata baria otozhennykh pri vysokich temperaturach (in Russian)*, *Iz. Akad. Nauk SSSR. Ser. Fiz.* **28**, 1964, 731-4.
- [11] MacChensky J.B., Potter J.E., *Factors and Mechanismus Affecting the Positive Temperature Coefficient of Resistivity of Barium Titanate*, *J. Am. Ceram. Soc.* **48**, 1965, 81-88.
- [12] Benguigui L., *Space Charge Limited Currents in BaTiO₃*, *Solid State Comm.* **7**, 1969, 1245-47.
- [13] Thomas R.T., *Time Dependence of the Electrical Conductivity of BaTiO₃ Single Crystal. Heated in Oxygen*, *J. Phys. D. Appl. Phys.* **3**, 1970, 1434-37.
- [14] Godefroy G., Coulson B., *Conductivity of BaTiO₃ Pure Single Crystals and Doped (Fe, OH) Single Crystals*, *J. Physique. CollC2.* **33**, 1972, 120-122.
- [15] Zabara Y.V., Kudzin A.Y., Kolesnichenko K.A., *Space-Charge-Limited Currents in Barium Titanate Single Crystals*, *Phys. Status Solidi (a)* **38**, 1976, K131-34.
- [16] Benguigui L., *Influence des électrodes sur les courants de charge d'espace dans le BaTiO₃ polycrystallin*, *Phys. Letts.* **25**, 1967, 117-8.
- [17] Osak W., Tkacz K., *Investigation of I-V Characteristics in Polycrystalline BaTiO₃*, *J. Phys. D. Appl. Phys.* **22**, 1989, 1746-50.
- [18] Andrich E., Hardt K.H., *Investigations on BaTiO₃ Semiconductors*, *Philips, Tech. Rev.* **26**, 1965, 119-27.
- [19] Kudzin L.Yu., Kolesnishesko K.A., Zabara Yu.V., *Space-Charge-Limited Currents in Semiconducting Barium Titanate (in Russian)*, *Izv. VUZ. Fiz.* **7**, 1976, 42-45.
- [20] Kolesnichenko K.A., Cherny B.K., Fedorova T.M., *Space-Charge-Limited Currents in Semiconducting Barium Titanate Ceramics with Various Donors Doped Concentration (in Russian)*, *Ukr. Fiz. Zhur.* **27**, 1982, 272-5.
- [21] Nemoto H., Oda J., *Direct Examinations of PTC Action of Single Grain Boundaries in Semiconducting BaTiO₃ Ceramics*, *J. Am. Ceram. Soc.* **63**, 1980, 398-401.
- [22] Mallick G.T., Emtage P.R., *Current-voltage Characteristics of Semiconducting Barium Titanate Ceramics.*, *J. Appl. Phys.* **39**, 1968, 3088-94.
- [23] Heywang W., *Bariumtitanat als Sperrschichtbleiter*, *Solid State Electronics* **3**, 1961, 51-58.

- [24] Heywang W., *Der Verlauf des Komplexen Widerstands von BaTiO₃-Halbleiter als Bestätigung des Sperschichtmodells* Zeit.f angew. Physik **16**, 1963, 1-5.
- [25] Heywang W., *Semiconducting Barium Titanate*, J. Mat. Science **6**, 1971, 1214-26.
- [26] Heywang W., *Resistivity Anomaly in Doped Barium Titanate*, J. Am. Ceram. Soc. **47**, 1964, 484-90.
- [27] Ihrig W., Puschert W., *A Systematic Experimental and Theoretical Investigation of the Grain-Boundary Resistivity of n-doped BaTiO₃ Ceramics*, J. Appl. Phys. **49**, 1977, 3081-88.
- [28] Hoffman B., *Ein Modell des Korngrenzenwiderstands in dotierter BaTiO₃-Keramik*, Solid State Electronics **16**, 1973, 623-28.
- [29] Jonscher A.K., *Dielectric Relaxation in Solids*, Ch. 6, Chelsea Dielectric Press London 1983.
- [30] van Turnhout J., *Thermally Stimulated Discharge Electrets*, Ch. 1, Elsevier, Amsterdam, New York 1975.
- [31] Lampert M.A., Mark P., *Current Injection in Solids*, Acad. Press, London 1970.
- [32] Kao K.C., Hwang W., *Electrical Transport in Solids*, Ch. 3-5, Pergamon Press, Oxford 1981.
- [33] Fridkin V.F., Kreher K., *Theory of Space-Charge-Limited Currents in Ferroelectrics*, Phys. Status Solidi (a) **2**, 1970, 281-5.
- [34] Krapivin V.F., Chensky E.V., *Space-Charge-Limited Currents in System Metal-Ferroelectrics-Metal (in Russian)*, Fiz. Tverd. Tela **12**, 1970, 597-604.
- [35] Osak W., Tkacz K., *Long-Lasting Relaxation Currents in TGS*, Phys. Status Solidi (a) **100**, 1987, 667-72.
- [36] Wieder H.H., *Retarded Polarisation Phenomena in BaTiO₃ Crystals*, J. Appl. Phys. **27**, 1956, 413-416.
- [37] Gurevich V.M., *Elektroprovodnos Segnetoelektrikov (in Russian)*, Izd. Stand. Mer., Moskva 1969.
- [38] Pollak M., *Temperature Dependence of a Hopping Conductivity*, Phys. Rev. **138**, 1965, 1822-1826.
- [39] Sayer M., Mansingh M.A., Webb J.B., Noad J., *Long-range Potential Centres in disordered Solids*, J. Phys. C. Solid State **11**, 1978, 315-329.
- [40] Charles R.J., *Polarisation and Diffusion in Silicate Glass*, J. Appl. Phys. **32**, 1961, 1115-1126.
- [41] Dyre J.C., *On the Mechanism of Glass Ionic Conductivity*, J. of Non-Crystalline Solids **88**, 1986, 271-280.